Paleoceanography and Paleoclimatology

RESEARCH ARTICLE
10.1029/2018PA003397

Influence of Model Bias on Simulating North Atlantic Sea Surface Temperature During the Mid-Pliocene

Zhaoyang Song[1], Mojib Latif[1,2], Wonsun Park[1], and Yuming Zhang[3]

[1]GEOMAR Helmholtz Centre for Ocean Research Kiel, Kiel, Germany, [2]Excellence Cluster "The Future Ocean" at Kiel University, Kiel, Germany, [3]National Marine Environmental Monitoring Center, State Oceanic Administration, Dalian, China

Key Points:
- We investigate the influence of alleviated North Atlantic cold sea surface temperature bias on the response of surface climate to closed gateways during the mid-Pliocene
- Alleviated cold sea surface temperature bias enhances ocean dynamical influences that strengthen the surface warming over the North Atlantic
- Model-proxy discrepancy is strongly reduced by alleviating cold sea surface temperature bias due to improved representation of mean North Atlantic Ocean circulation

Supporting Information:
- Supporting Information S1

Correspondence to:
Z. Song,
zsong@geomar.de

Citation:
Song, Z., Latif, M., Park, W., & Zhang, Y. (2018). Influence of model bias on simulating North Atlantic sea surface temperature during the mid-Pliocene. *Paleoceanography and Paleoclimatology*, *33*, 884–893. https://doi.org/10.1029/2018PA003397

Received 30 APR 2018
Accepted 5 JUL 2018
Accepted article online 11 JUL 2018
Published online 20 AUG 2018

Abstract Climate models generally underestimate the pronounced warming in the sea surface temperature (SST) over the North Atlantic during the mid-Pliocene that is suggested by proxy data. Here we investigate the influence of the North Atlantic cold SST bias, which is observed in many climate models, on the simulation of mid-Pliocene surface climate in a series of simulations with the Kiel Climate Model. A surface freshwater-flux correction is applied over the North Atlantic, which considerably improves simulation of North Atlantic Ocean circulation and SST under present-day conditions. Using reconstructed mid-Pliocene boundary conditions with closed Bering and Arctic Archipelago Straits, the corrected model depicts significantly reduced model-proxy SST discrepancy in comparison to the uncorrected model. A key factor in reducing the discrepancy is the stronger and more sensitive Atlantic Meridional Overturning Circulation and poleward heat transport. We conclude that simulations of mid-Pliocene surface climate over the North Atlantic can considerably benefit from alleviating model biases in this region.

1. Introduction

The mid-Pliocene, from 3.264 to 3.025 million years before present, is the most recent geological period when the atmospheric CO_2 concentration was comparable to the present-day concentration. Yet the globally averaged surface temperature was significantly warmer (Fedorov et al., 2013; Martínez-Botí et al., 2015). Therefore, the mid-Pliocene may offer insights into the surface warming during the mid-21st century (Zubakov & Borzenkova, 1988). Both marine and terrestrial reconstructions suggest that the tropical surface temperatures only exhibited minor differences to the present-day temperatures but the high latitudes, particularly the subpolar North Atlantic and the Atlantic sector of the Arctic, were much warmer (e.g., Dowsett et al., 1996; Thompson & Fleming, 1996). However, climate model simulations from the Pliocene Model Intercomparison Project phase 1 fail to reproduce the pronounced warming over the North Atlantic (Haywood et al., 2016).

Several hypotheses have been offered to explain the discrepancy between the models and the proxy data (Figure 1a; proxy data in Table S1 by Dowsett et al., 2012, 2013). For example, uncertainties in the boundary conditions or climate model deficiencies have been proposed (e.g., Crowley, 1991; Hill, 2015; Otto-Bliesner et al., 2017; Unger & Yue, 2014). Based on temperature reconstructions, enhanced poleward ocean heat transport associated with a strengthened Atlantic Meridional Overturning Circulation (AMOC) has been proposed to explain the large warming over the North Atlantic (Dowsett et al., 1992). Hill (2015) investigates the AMOC response to the individual and combined impacts of rerouted river runoff from the North American and Baltic rivers, lowering Greenland-Scotland ridge and replacing the Barents Sea with landmass. Only the lowering of the Greenland-Scotland ridge supports an enhanced AMOC, yet it is unable to produce the strong warming over the North Atlantic. Dowsett et al. (2016) proposed closed Bering and Arctic Archipelago Straits in the most recently updated version of the boundary condition data set for the mid-Pliocene. The closure of these Arctic gateways could result in much enhanced AMOC and substantially reduce the model-data discrepancies in the North Atlantic (Otto-Bliesner et al., 2017). Moreover, the role of cloud albedo on simulating the Pliocene climate has been addressed with a suite of climate model simulations (Burls & Fedorov, 2014). However, the influence of the North Atlantic cold sea surface temperature (SST) bias has not been explored in detail.

Most climate models participating in the Coupled Model Intercomparison Project phase 5 (Taylor et al., 2012) suffer from a significant cold SST bias in the North Atlantic (Figure S1 in the supporting information), which generally originates from the biased mean ocean circulation such as a too weak AMOC or an incorrect path of

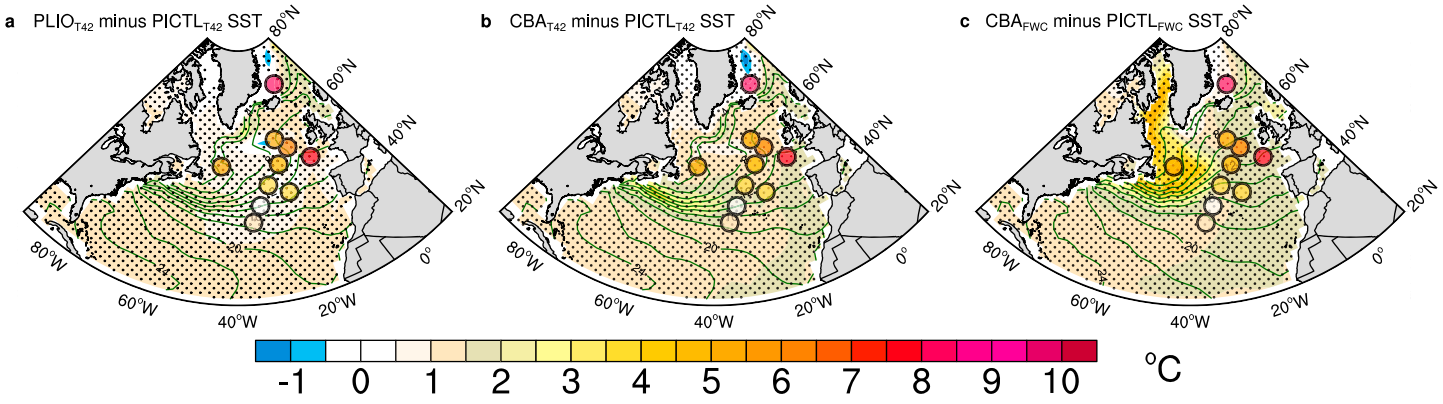

Figure 1. Response of annual mean sea surface temperature (SST, unit: °C) to (a) increased CO_2 and (b) closed Bering and Arctic Archipelago Straits and increased CO_2 in the standard Kiel Climate Model (T42). (c) As in (b) but from the freshwater flux-corrected Kiel Climate Model version (FWC). Green contours depict climatological mean SST (contour interval: 2 °C) in (a, b) T42 and (c) FWC. Stippling indicates statistical significance at the 95% confidence level using Student's *t* test.

the North Atlantic Current (Park et al., 2016; Scaife et al., 2011; Wang et al., 2014). The deficient oceanic heat and salinity transports among others alter the stratification and therefore misplace the deep convection sites in the North Atlantic (Drews et al., 2015; Park et al., 2016). Furthermore, the positive feedback between the AMOC strength and the density in the middle- and high-latitude North Atlantic (Hofmann & Rahmstorf, 2009) strongly amplifies the biases in the mean ocean circulation and surface climate over the North Atlantic. As a consequence, the response of the Atlantic ocean circulation and North Atlantic surface climate to changes in ocean gateways and rivers routes could be biased as well (e.g., Hill, 2015; Otto-Bliesner et al., 2017).

Here we use the Kiel Climate Model (KCM; Park et al., 2009) to investigate the influence of model biases in the North Atlantic on the ocean circulation and surface climate response to closed Bering and Arctic Archipelago Straits during the mid-Pliocene. Two versions of the KCM are employed in this study: the original version exhibiting large upper ocean salinity and temperature biases in the North Atlantic, specifically a large North Atlantic cold SST bias, and a version with much reduced biases. Bias reduction is achieved by applying a surface freshwater flux correction over the North Atlantic (Park et al., 2016). The enhanced simulation of North Atlantic salinities improves the representation of the ocean circulation in the Atlantic, especially the AMOC, which in turn improves the simulation of North Atlantic SSTs.

The paper is organized as follows: Section 2 describes the climate model and the experimental setup. We explore the influence of model bias on the response to the closed Bering and Arctic Archipelago Straits in section 3. Summary and Discussion are presented in section 4 and conclude the paper.

2. Model and Experimental Design

The KCM is a fully coupled atmosphere-ocean-sea ice general circulation model. Its atmospheric model is ECHAM5 (Roeckner et al., 2003) with a horizontal resolution of T42 (2.8° × 2.8°) and 19 vertical levels up to 10 hPa. The ocean-sea ice component is NEMO (Madec, 2008) on a 2° Mercator mesh, with 31 vertical levels. The meridional resolution enhances toward lower latitudes, with 0.5° in the equatorial region. The two components are coupled with the OASIS3 coupler (Valcke, 2006). The standard KCM does not employ any form of flux correction or anomaly coupling and suffers from a large cold SST biases up to 8 °C in the North Atlantic (Figure 2a). Following Park et al. (2016) a surface freshwater-flux correction over the North Atlantic (Figure S2) is applied to the KCM, which, by definition, substantially reduces sea surface salinity (SSS) biases in this region (Figure 3b). Application of the surface freshwater-flux correction also substantially reduces the cold SST bias over the North Atlantic (Figure 2b).

Two sets of simulations (Table 1) with the standard (labeled **T42**) and freshwater-flux corrected KCM (labeled **FWC**) are performed. Each set consists of three experiments: one 1,000-year-long control integration (**PICTL**) that is initialized with the Levitus climatology of temperature and salinity. The control integration employs the modern (open) Bering and Arctic Archipelago Straits with atmospheric CO_2 concentration fixed at 286

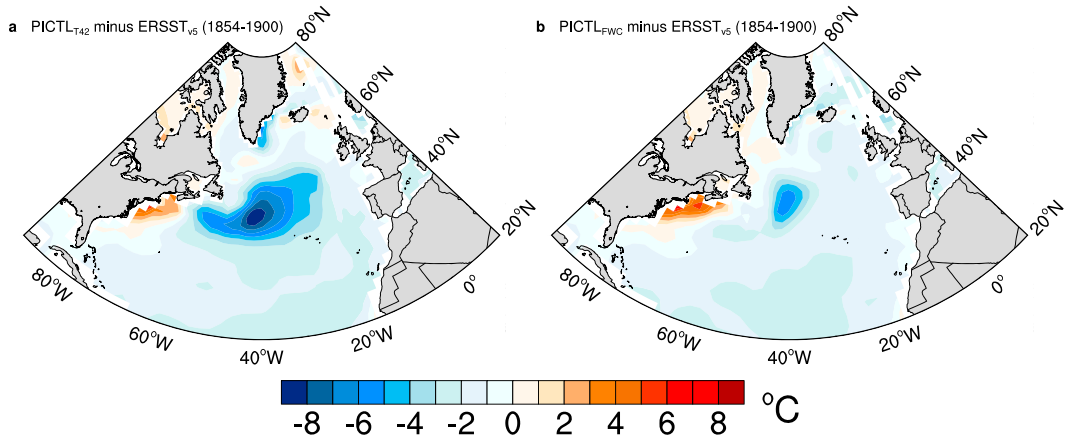

Figure 2. The annual mean SST biases (unit: °C) for the (a) standard Kiel Climate Model (KCM; T42) and (b) freshwater flux-corrected KCM version (FWC). The bias is calculated as the difference between the simulated SST and the ERSST$_{v5}$ (https://www.ncdc.noaa.gov/data-access/marineocean-data/extended-reconstructed-sea-surface-temperature-ersst-v5).

parts per million by volume. In the second experiment (**PLIO**) only the atmospheric CO_2 concentration is increased to 405 ppm following the PlioMIP protocol (Haywood et al., 2011). The orography, vegetation, and ice sheet mask implemented in **PLIO** are the same as in **PICTL**. Based on the latest Pliocene Research, Interpretation and Synoptic Mapping (PRISM4) reconstruction data set (Dowsett et al., 2016, and references therein), ***c***losed ***B***ering and Arctic ***A***rchipelago Straits are implemented in the third experiment (**CBA**). In **CBA**, atmospheric CO_2 is also fixed at 405 ppm.

Apart from **PICTL$_{T42}$**, all simulations are integrated for 800 years and the monthly mean output of the last 300 years is taken for analysis (Figure S3). Initialization is as follows; **PLIO$_{T42}$**, **CBA$_{T42}$**, and **PICTL$_{FWC}$** start from conditions at year 500 of **PICTL$_{T42}$**. **PLIO$_{FWC}$** and **CBA$_{FWC}$** start from year 500 of **PICTL$_{FWC}$**.

3. Results

3.1. Response to Seaway Changes

We first discuss the response of annual mean SSS to the closed Bering and Arctic Archipelago Straits. The closed Bering and Archipelago straits generally increase the SSS in the North Atlantic. However, the response patterns are rather different among the two KCM versions (Figures 4a and 4b). In the uncorrected model (T42), the closure of the straits results in increased SSS of up to 1.4 psu in a zonal band at 40°N extending into

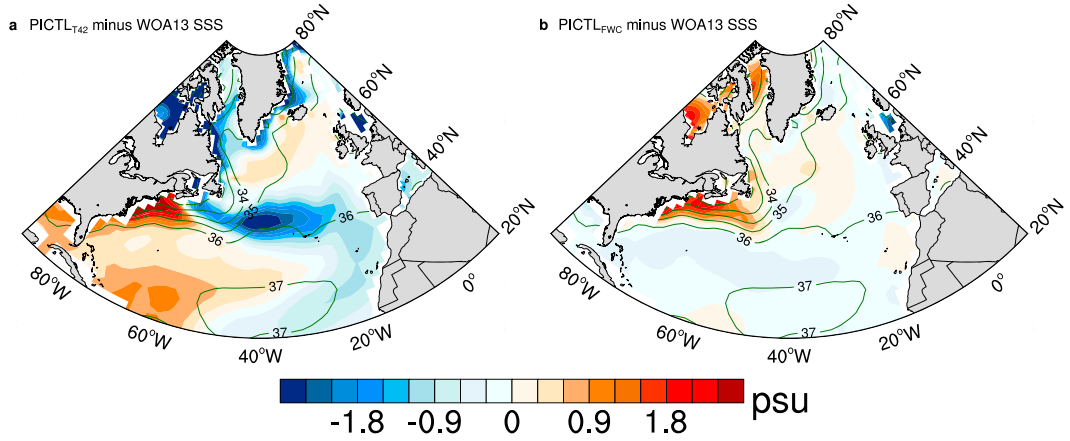

Figure 3. SSS biases (unit: psu) in a T42 and (b) FWC in relative to the World Ocean Atlas 2013 (WOA13) data (https://www.nodc.noaa.gov/OC5/woa13/woa13data.html). Green contours (contour interval: 1 psu) show the climatological annual mean SSS of the WOA13.

Table 1
Overview of the Model Simulations Analyzed in This Paper

Experiment name	Flux correction	Atmospheric CO_2 (ppm)	Bering and Arctic Archipelago Straits	Integration time (model years)
$PICTL_{T42}$	Without	286	Open	1,000
$PLIO_{T42}$	Without	405	Open	800
CBA_{T42}	Without	405	Closed	800
$PICTL_{FWC}$	With	286	Open	800
$PLIO_{FWC}$	With	405	Open	800
CBA_{FWC}	With	405	Closed	800

Note. **PLIO** and **CBA** are based on PRISM3 (Haywood et al., 2011) and PRISM4 (Dowsett et al., 2016) Bering and Arctic Archipelago Straits conditions, respectively. Subscripts T42 and FWC indicate the KCM with and without applying a surface freshwater-flux correction over the North Atlantic, respectively.

the eastern North Atlantic (Figure 4a). Further, the SSS increases in the Baffin Bay, which is mainly due to the reduced freshwater transport by 0.14 Sv. In contrast, the SSS decreases in the Greenland-Iceland-Norwegian (GIN) seas owing to the weakened salinity transport (not shown). This is consistent with the CCSM4 modeling results by Otto-Bliesner et al. (2017). The flux-corrected model (FWC), on the other hand, only simulates increased salinity in the western North Atlantic, in the Labrador Sea and west of Greenland (including the Baffin Bay; Figure 4b). In particular, the salinity increase in the western North Atlantic in FWC amounts to 1.6 psu as compared to 0.6 psu in T42.

The SSS changes due to the closed straits drive marked changes in the deep water formation in the subpolar North Atlantic. The winter mean (December to February) mixed layer depth (MLD) is a measure of deep convection in this region (Figures 4c and 4d). The MLD is defined as the depth at which the density increases from the ocean surface by 0.01 kg/m^3. As shown by the contours in Figure 4c, the deep convection sites in T42 are located south of Greenland, in the Irminger Sea and GIN Sea. The convection site south of Greenland shifts westward into the Labrador Sea in FWC (contours in Figure 4d), which is more realistic with respect to present-day conditions

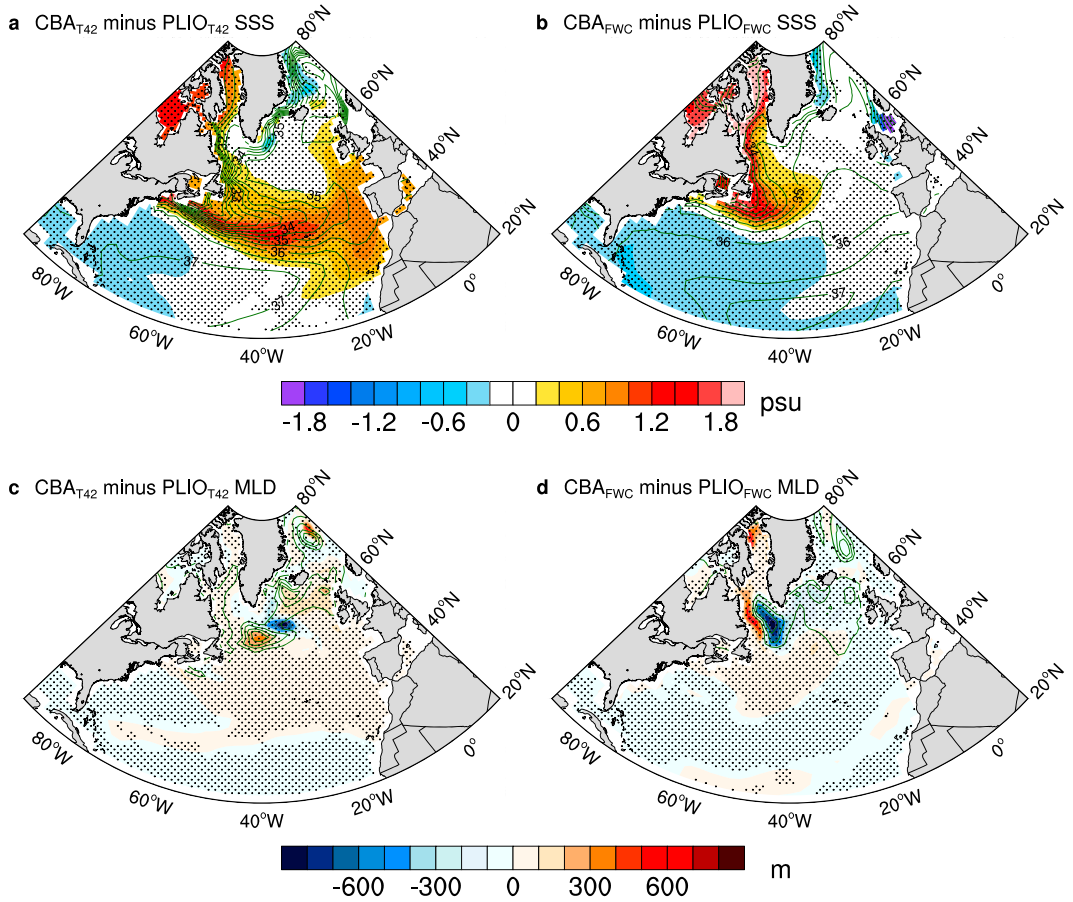

Figure 4. Response of annual mean sea surface salinity (SSS, unit: psu) to closed Bering and Arctic Archipelago Straits in (a) T42 and (b) FWC. Green contours depict climatological mean SSS (contour interval: 0.5 psu). Response of DJF (December–February) mean mixed layer depth (MLD, unit: m) to closed Bering and Arctic Archipelago straits in (c) T42 and d FWC. Green contours depict climatological DJF mean MLD (contour interval: 400 m). Stippling indicates statistical significance at the 95% confidence level using Student's *t* test.

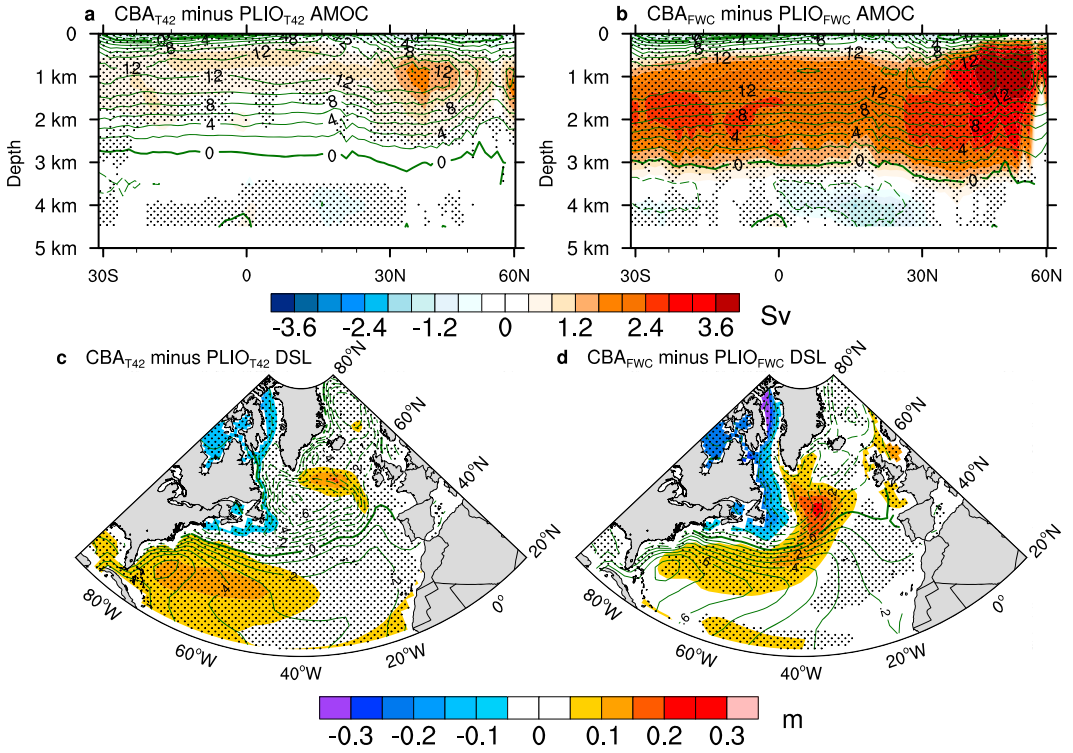

Figure 5. Response of annual mean Atlantic Meridional Overturning Circulation (AMOC, unit: Sv) to closed Bering and Arctic Archipelago Straits in (a) T42 and (b) FWC. Green contours depict climatological mean AMOC (contour interval: 2 Sv). Response of annual mean dynamic sea level (DSL, unit: m) to closed Bering and Arctic Archipelago Straits in (c) T42 and (d) FWC. Green contours depict climatological mean DSL (contour interval: 0.1 m). Stippling indicates statistical significance at the 95% confidence level using Student's *t* test.

(Figure S4). With the closure of Bering and Arctic Archipelago Straits, a dipole response in the deep convention region south of Greenland is observed in T42 (color shading in Figure 4c). The MLD averaged in the domain of GIN Sea (66°N to 78°N, 6°W to 12°E) also deepens from 132 m in PLIO$_{T42}$ to 149 m in CBA$_{T42}$. In FWC, a much stronger dipole response of MLD is simulated in the Labrador Sea with shoaling MLD in the east and deepening MLD in the west. The MLD also increases in the Baffin Bay, while it hardly changes in the GIN Sea.

The intensified deep convection due to the closed gateways drives a stronger AMOC in both integrations (Figures 5a and 5b). The AMOC strength, defined as the maximum overturning stream function at 30°N, increases from 12.4 Sv in PLIO$_{T42}$ to 13.4 Sv in CBA$_{T42}$ (Figure 5a). Accordingly, the associated meridional oceanic heat transport averaged over the latitude range 40°N and 60°N slightly increases from 0.35 PW in PLIO$_{T42}$ to 0.38 PW in CBA$_{T42}$ (not shown). The corrected model FWC yields a larger increase in AMOC strength from 14.1 Sv in PLIO$_{FWC}$ to 16.3 Sv in CBA$_{FWC}$ (Figure 5b). Further, the meridional oceanic heat transport averaged over the latitude range 40°N and 60°N increases from 0.37 PW in PLIO$_{FWC}$ to 0.48 PW in CBA$_{FWC}$ (not shown). This relative change (30%) in the heat transport is much stronger than that (10%) reported by Otto-Bliesner et al. (2017).

As shown by Park et al. (2016), the mean horizontal circulation is less biased in comparison with satellite observations when applying the freshwater correction. The annual-mean dynamic sea level (DSL), defined as the sea surface height deviation from the globally averaged sea surface height, illustrates the mean horizontal circulation (contours in Figures 5c and 5d). Compared to the DSL in T42 (contours in Figure 5c), FWC exhibits a steeper DSL gradient at 40°N in the western North Atlantic, which implies a stronger Gulf Stream. Additionally, the path of the North Atlantic Current is farther northward reaching (contours in Figure 5d) and the subpolar gyre less extensive in FWC.

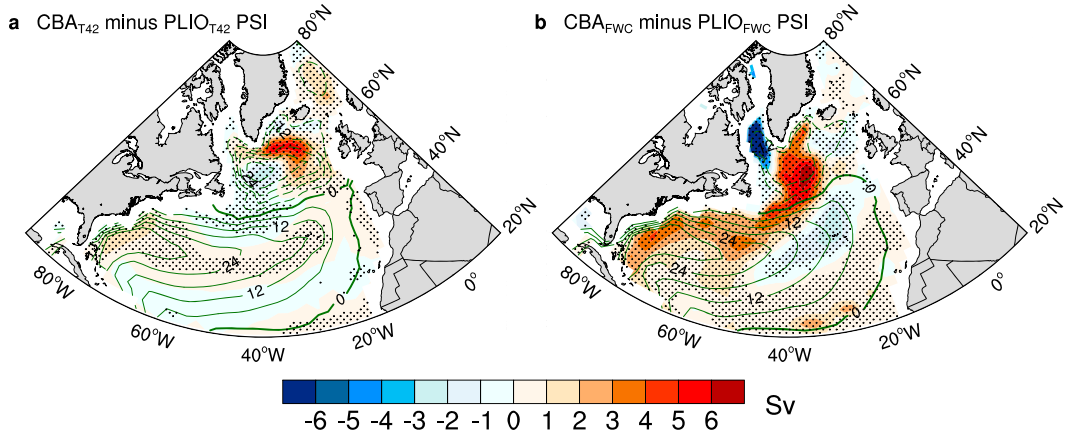

Figure 6. Responses of annual mean barotropic stream function (shading, unit: Sv) to closed Bering and Arctic Archipelago Straits are depicted in (a) T42 and (b) FWC. Green contours show climatological mean stream function (contour interval: 6 Sv) for (a) T42 and (b) FWC. Positive differences and solid contours indicate clockwise circulation and vice versa for the negative differences and dashed contours. Stippling indicates the responses are statistically significant at the 95% confidence level using Student's *t* test.

The DSL response to the closed gateways in FWC (Figure 5d) is rather different to that in T42 (Figure 5c). The negative DSL signals in the Baffin Bay and west of Greenland are much stronger and the positive DSL signals stretch more northward in comparison to those in T42 (Figure 5d). As illustrated by the barotropic stream function, the Gulf Stream in FWC intensifies by 4 Sv as opposed to 1 Sv in T42 (Figures 6a and 6b). Over the midlatitude North Atlantic, the closed straits slightly increase the DSL by up to 0.22 m at the northeastern flank of the subpolar gyre in T42 (Figure 5a). The subpolar gyre strength, defined as the barotropic stream function averaged over 50°N to 58°N, 26°W to 42°W, weakens from 25.25 Sv in PLIO$_{T42}$ to 23.75 Sv in CBA$_{T42}$ (Figure 6a). A stronger response is observed in FWC, which features an increase in DSL of up to 0.25 m (Figure 5d) and decrease in subpolar gyre strength of 3.8 Sv (Figure 6b).

The mismatch between the SST proxies and the model is much reduced in FWC (Figures 1b and 1c). We quantify this mismatch with the root-mean-square error metric. The root-mean-square error over the North Atlantic (40°N to 60°N) decreases from 4.93 °C in CBA$_{T42}$ to 4.41 °C in CBA$_{FWC}$. Relative to the preindustrial control experiment, the closed ocean gateways and high atmospheric CO_2 concentration induce a warming of 1.2 °C averaged over the midlatitude North Atlantic in T42 (Figure 1b). In particular, the Gulf Stream region features warming of up to 4.1 °C while east of Greenland, cooling of 1.5 °C is simulated. The warming is greatly amplified in FWC, especially in the western North Atlantic, the Labrador Sea, and Baffin Bay (Figure 1c). Further, the warming signal in the east expands westward and northward. In the GIN Sea, however, which is the region of the largest warming according to the proxy data, no improvement is achieved. Overall, the surface freshwater flux correction applied to the model not only improves the representation of the mean Atlantic Ocean circulation and North Atlantic SST but also enhances their sensitivity to closing the Bering and Arctic Archipelago Straits.

3.2. Mechanism for the Response

A heat budget analysis is applied to quantify the contributions of the surface heat flux and ocean dynamical heating processes. Following DiNezio et al. (2009) and Salau et al. (2012), the heat budget over the upper 300 m (*H*) can be expressed as

$$\frac{\partial Q}{\partial t} = Q_{net} + Q_{dyn} + Q_{SCS}, \quad (1)$$

where Q_{net} is the net surface heat flux defined by the sum of sensible heat flux, latent heat flux, shortwave radiation, and longwave radiation. Q_{dyn} denotes the overall contributions of zonal (Q_u), meridional (Q_v), and vertical (Q_w) advective heating by resolved ocean currents using

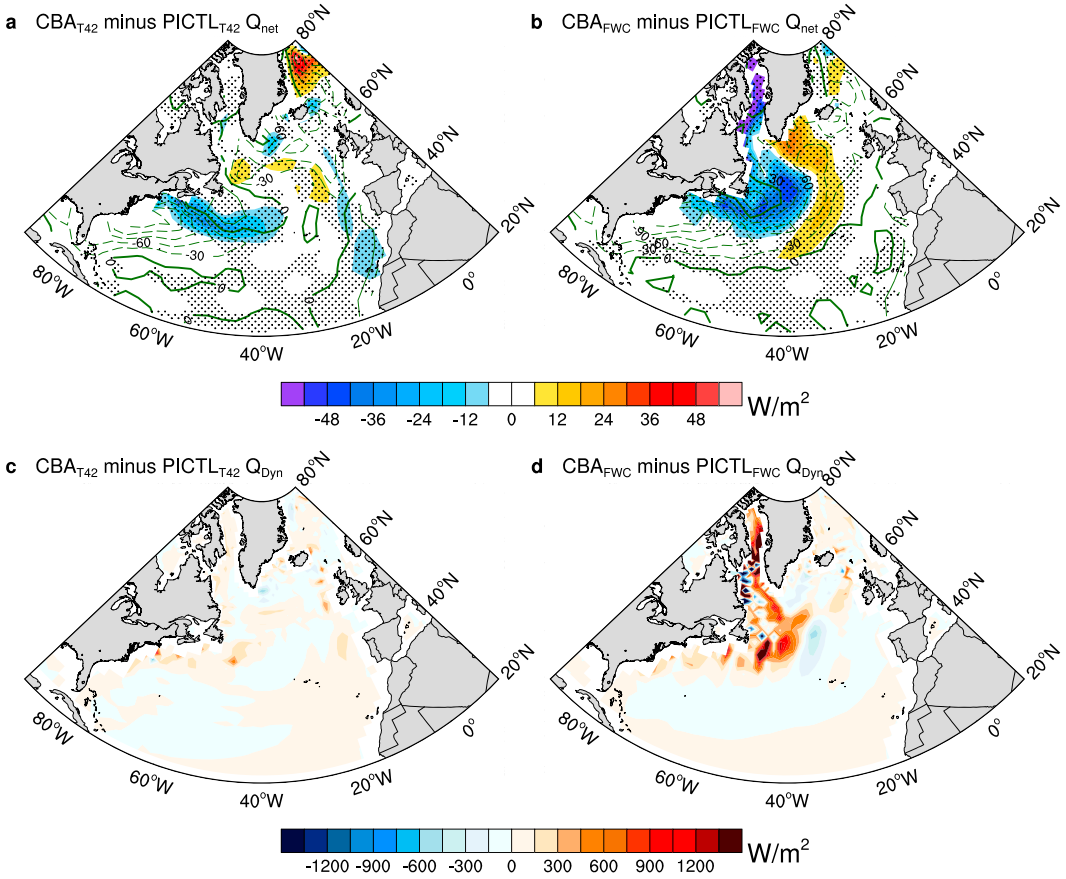

Figure 7. Response of annual mean net surface heat flux (Q_{net}, unit: W/m^2) to closed Bering and Arctic Archipelago Straits and higher CO_2 in (a) T42 and (b) FWC. Green contours depict climatological mean Q_{net} (contour interval: 30 W/m^2). Solid contours and positive color shadings indicate that the ocean gains heat from the atmosphere, and vice versa. Stippling indicates statistical significance at the 95% confidence level using Student's *t* test. Response of annual mean ocean dynamical heating (Q_{dyn}, unit: W/m^2), vertically integrated over the upper 300 m, to closed Bering and Arctic Archipelago Straits and higher CO_2 in (c) T42 and (d) FWC.

$$Q_u = \rho c_p \int_{-H}^{0} u \frac{\partial T}{\partial x} dz, \tag{2}$$

$$Q_v = \rho c_p \int_{-H}^{0} v \frac{\partial T}{\partial y} dz, \tag{3}$$

$$Q_w = \rho c_p \int_{-H}^{0} w \frac{\partial T}{\partial z} dz. \tag{4}$$

Q_{SCS} is the ocean heat transport by unresolved processes, which is neglected here. ρ and c_p are the density specific heat capacity of water, respectively. The product of ρ and c_p equals $4.1 \times 10^6 J \cdot m^{-3} \cdot K^{-1}$.

Relative to the preindustrial control experiment, the response of Q_{net} to the closed straits and higher CO_2 in T42 depicts a damping on the SSTs in the Gulf Stream region where the ocean loses heat to the atmosphere (Figure 7a). In the midlatitude North Atlantic, however, there are no large changes in the surface heat flux. Heat is gained from the atmosphere in the GIN Sea (Figure 7a), where SSTs exhibit slight cooling (Figure 1b). The response of Q_{net} in FWC is rather different. Oceanic heat loss is observed over the Gulf Stream region, western North Atlantic, parts of the subpolar gyre, and west of Greenland (Figure 7b). Heat loss indicates a damping on the SSTs in the aforementioned regions. On the other hand, the Irminger Sea and the GIN Sea receive heat from the atmosphere.

With closed Bering and Arctic Archipelago Straits and high CO_2, slightly enhanced ocean dynamical heating only is found in scattered regions of the North Atlantic and Arctic in T42 (Figure 7c). The change in total ocean

dynamical heating Q_{dyn} amounts to 35.6 W/m^2 averaged over the latitude range 40°N to 60°N. The individual dynamical heating terms are shown in (Figures S5a, S5c, and S5e). In contrast, much stronger changes in dynamical heating are observed in FWC (Figure 7d). The averaged Q_{dyn} over the latitude range 40°N to 60°N is 240.7 W/m^2. Increased total dynamical heating is observed in the western North Atlantic, in the Labrador Sea and Baffin Bay, and west of Greenland (Figure 7d). The meridional dynamical heating term is by far the largest contribution (Figure S5d). Zonal dynamical heating is important in the Gulf Stream region, subpolar gyre and Baffin Bay, zonal dynamical cooling in the Labrador Sea, and off Newfoundland (Figure S5b). The changes in vertical dynamical heating are mostly negligible (Figure S5f). Our results support the hypothesis that the warm North Atlantic climate during the mid-Pliocene may be, at least partly, the result of increased ocean heat transports due to an enhanced thermohaline circulation and more realistic gyre circulation (Raymo et al., 1989; Rind & Chandler, 1991).

4. Summary and Discussion

This study investigates the influence of model biases on the ocean circulation and surface climate of the North Atlantic during the mid-Pliocene by conducting a series of experiments with the KCM. The KCM's response to closed Bering and Arctic Archipelago Straits and increased atmospheric CO_2 concentration was studied with the standard KCM (T42) and a version in which a surface freshwater-flux correction is applied over the North Atlantic (FWC). The latter version exhibits considerably reduced biases with respect to the Atlantic Ocean circulation and North Atlantic SSS and SST. Model-proxy SST discrepancy over large regions of the North Atlantic and Artic is substantially reduced in the FWC, particularly in the west. This is largely due to much enhanced ocean dynamical heating, with the meridional component contributing the largest share.

We note that the proxy evidence for stronger poleward heat transport in the North Atlantic during the mid-Pliocene is still under debate. It has been suggested that the AMOC gradually strengthened as the closure of the Panama Seaway increased the salinity in the Atlantic (Bartoli et al., 2005; Haug & Tiedemann, 1998; Haug et al., 2001; Maier-Reimer et al., 1990; Zhang et al., 2012). However, the exact timing for the final closure of the Panama Seaway remains unclear (e.g., Molnar, 2008; Montes, 2015). Mestas-Nuñez and Molnar (2014) pointed that the increased salinity contrast between the Pacific and Atlantic could be explained by the reduced atmospheric moisture transport due to a warmer eastern tropical Pacific. Numerous studies present evidence for a stronger AMOC during the mid-Pliocene relative to present-day conditions, which among others (e.g., Frank et al., 2002; Frenz et al., 2006) is supported by a weaker north-south $\delta^{13}C$ gradient in the Atlantic (Ravelo & Andreasen, 2000; Raymo et al., 1996). However, climate models from the Pliocene Model Intercomparison Project phase 1 do not simulate a stronger AMOC, when forced by mid-Pliocene boundary conditions without the Arctic gateway changes. Zhang et al. (2013) suggested that the weak north-south $\delta^{13}C$ gradient could be due to either the increased ventilation or reduced stratification in the Southern Ocean. Additionally, the existence of a Pacific Meridional Overturning Circulation in the north Pacific may also account for the weak $\delta^{13}C$ gradient (Burls et al., 2017).

We note that the flux-corrected KCM, with the implementation of the two closed ocean gateways, still substantially underestimates the SST in the GIN Sea (Figure 1c). A previous study has illustrated that the sea ice is a crucial climate system component for the simulation of the SSTs in the Arctic (Howell et al., 2016). However, the flux-correction applied to the KCM fails to improve the sea ice extent east of Greenland (Park et al., 2016). In FWC, even larger sea ice extent is simulated in response to the two closed straits (Figure S6). Moreover, the lack of terrestrial ecosystem greenhouse gas emissions and interactive chemistry-climate feedbacks may contribute to the erroneous response (Unger & Yue, 2014).

The use of flux correction/adjustment to investigate climate change is still under debate. For instance, theoretical studies have suggested that the AMOC can have more than one stable state (Stommel, 1961). However, even state-of-the-art coupled climate models in the Coupled Model Intercomparison Project phase 5 are biased toward a monostable AMOC, which may be attributed to the surface climate biases, especially in the tropical and northern North Atlantic (Liu et al., 2014). Using large flux adjustment, Manabe and Stouffer (1988) were the first to investigate a bistable behavior of the AMOC in a coupled climate model, thus explaining the abrupt climate changes observed in paleoclimate records. Moreover, Liu et al. (2017) simulates a collapsed AMOC under global warming with a flux-corrected model, as compared to modest changes in the

AMOC in most other climate model projections. Gent (2017) argued that the flux correction does not only improve the mean surface climate but also strongly interfere with the associated ocean-atmosphere feedbacks, thus significantly affecting the AMOC stability properties. Therefore, the conclusions drawn from flux-adjusted models should be interpreted with caution.

We conclude that alleviating model biases may enable coupled climate models to more realistically simulate the response of the surface climate over the North Atlantic to closed Bering and Arctic Archipelago Straits during the mid-Pliocene. As enhancing the horizontal model resolution does not necessarily improve model performance in the North Atlantic (Delworth et al., 2012; Griffies et al., 2015), the application of a regional flux correction that improves the Atlantic salinity distribution may serve as an interim solution to enhance paleoclimate modeling with altered boundary conditions.

Acknowledgments
We thank Natalie Burls and another anonymous reviewer for their helpful comments. This study was supported by the Integrated School of Ocean Sciences (ISOS) at the Excellence Cluster "The Future Ocean" at Kiel University sponsored by the German Science Foundation (DFG). We thank Taewook Park for his helpful comments. The simulations with the Kiel Climate Model (KCM) were conducted at the Computing Center of Kiel University. The KCM results presented in this study are available at https://doi.pangaea.de/10.1594/PANGAEA.889380. Yuming Zhang is supported by the National Natural Science Foundation of China (grant 41606002) and the Key Laboratory of Global Change and Marine-Atmospheric Chemistry (GCMAC1308). This is a contribution to PalMod.

References

Bartoli, G., Sarnthein, M., Weinelt, M., Erlenkeuser, H., Garbe-Schönberg, D., & Lea, D. W. (2005). Final closure of Panama and the onset of northern hemisphere glaciation. *Earth and Planetary Science Letters*, *237*(1-2), 33–44. https://doi.org/10.1016/j.epsl.2005.06.020

Burls, N. J., & Fedorov, A. V. (2014). What controls the mean east–west sea surface temperature gradient in the equatorial Pacific: The role of cloud albedo. *Journal of Climate*, *27*(7), 2757–2778. https://doi.org/10.1175/JCLI-D-13-00255.1

Burls, N. J., Fedorov, A. V., Sigman, D. M., Jaccard, S. L., Tiedemann, R., & Haug, G. H. (2017). Active Pacific meridional overturning circulation (PMOC) during the warm Pliocene. *Science Advances*, *3*(9), e1700156. https://doi.org/10.1126/sciadv.1700156

Crowley, T. J. (1991). Modeling Pliocene warmth. *Quaternary Science Reviews*, *10*(2–3), 275–282. https://doi.org/10.1016/0277-3791(91)90025-P

Delworth, T. L., Rosati, A., Anderson, W., Adcroft, A. J., Balaji, V., Zhang, R., et al. (2012). Simulated climate and climate change in the GFDL CM2.5 high-resolution coupled climate model. *Journal of Climate*, *25*(8), 2755–2781. https://doi.org/10.1175/JCLI-D-11-00316.1

DiNezio, P. N., Clement, A. C., Vecchi, G. A., Soden, B. J., Kirtman, B. P., & Lee, S. K. (2009). Climate response of the equatorial Pacific to global warming. *Journal of Climate*, *22*(18), 4873–4892. https://doi.org/10.1175/2009JCLI2982.1

Dowsett, H., Barron, J., & Poore, R. (1996). Middle Pliocene sea surface temperatures: A global reconstruction. *Marine Micropaleontology*, *27*(1–4), 13–25. https://doi.org/10.1016/0377-8398(95)00050-X

Dowsett, H., Dolan, A., Rowley, D., Moucha, R., Forte, A. M., Mitrovica, J. X., et al. (2016). The PRISM4 (mid-Piacenzian) paleoenvironmental reconstruction. *Climate and Pastoralism*, *12*(7), 1519–1538. https://doi.org/10.5194/cp-12-1519-2016

Dowsett, H. J., Cronin, T. M., Poore, R. Z., Thompson, R. S., Whatley, R. C., & Wood, A. M. (1992). Micropaleontological evidence for increased meridional heat transport in the North Atlantic Ocean during the Pliocene. *Science*, *258*(5085), 1133–1135. https://doi.org/10.1126/science.258.5085.1133

Dowsett, H. J., Foley, K. M., Stoll, D. K., Chandler, M. A., Sohl, L. E., Bentsen, M., et al. (2013). Sea surface temperature of the mid-Piacenzian Ocean: A data-model comparison. *Scientific Reports*, *3*(1). https://doi.org/10.1038/srep02013

Dowsett, H. J., Robinson, M. M., Haywood, A. M., Hill, D. J., Dolan, A. M., Stoll, D. K., et al. (2012). Assessing confidence in Pliocene sea surface temperatures to evaluate predictive models. *Nature Climate Change*, *2*(5), 365. https://doi.org/10.1038/nclimate1455

Drews, A., Greatbatch, R. J., Ding, H., Latif, M., & Park, W. (2015). The use of a flow field correction technique for alleviating the North Atlantic cold bias with application to the Kiel Climate Model. *Ocean Dynamics*, *65*(8), 1079–1093. https://doi.org/10.1007/s10236-015-0853-7

Fedorov, A. V., Brierley, C. M., Lawrence, K. T., Liu, Z., Dekens, P. S., & Ravelo, A. C. (2013). Patterns and mechanisms of early Pliocene warmth. *Nature*, *496*(7443), 43–49. https://doi.org/10.1038/nature12003

Frank, M., Whiteley, N. S., Kasten, S., Hein, J. R., & O'Nions, K. (2002). North Atlantic deep water export to the Southern Ocean over the past 14 Myr: Evidence from Nd and Pb isotopes in ferromanganese crusts. *Paleoceanography*, *17*(2), 1022. https://doi.org/10.1029/2000PA000606

Frenz, M., Henrich, R., & Zychla, B. (2006). Carbonate preservation patterns at the Ceará Rise—Evidence for the Pliocene super conveyor. *Marine Geology*, *232*(3-4), 173–180. https://doi.org/10.1016/j.margeo.2006.07.006

Gent, P. R. (2017). A commentary on the Atlantic meridional overturning circulation stability in climate models. *Ocean Modelling*, *122*, 57–66. https://doi.org/10.1016/j.ocemod.2017.12.006

Griffies, S. M., Winton, M., Anderson, W. G., Benson, R., Delworth, T. L., Dufour, C. O., et al. (2015). Impacts on ocean heat from transient mesoscale eddies in a hierarchy of climate models. *Journal of Climate*, *28*(3), 952–977. https://doi.org/10.1175/JCLI-D-14-00353.1

Haug, G. H., & Tiedemann, R. (1998). Effect of the formation of the Isthmus of Panama on Atlantic Ocean thermohaline circulation. *Nature*, *393*(6686), 673–676. https://doi.org/10.1038/31447

Haug, G. H., Tiedemann, R., Zahn, R., & Ravelo, A. C. (2001). Role of Panama uplift on oceanic freshwater balance. *Geology*, *29*(3), 207–210. https://doi.org/10.1130/0091-7613(2001)029<0207:ROPUOO>2.0.CO;2

Haywood, A. M., Dowsett, H. J., Dolan, A. M., Rowley, D., Abe-Ouchi, A., Otto-Bliesner, B., et al. (2016). The Pliocene Model Intercomparison Project (PlioMIP) phase 2: Scientific objectives and experimental design. *Climate and Pastoralism*, *12*(3), 663–675. https://doi.org/10.5194/cp-12-663-2016

Haywood, A. M., Dowsett, H. J., Robinson, M. M., Stoll, D. K., Dolan, A. M., Lunt, D. J., et al. (2011). Pliocene Model Intercomparison Project (PlioMIP): Experimental design and boundary conditions (Experiment 2). *Geoscientific Model Development*, *4*(3), 571–577. https://doi.org/10.5194/gmd-4-571-2011

Hill, D. J. (2015). The non-analogue nature of Pliocene temperature gradients. *Earth and Planetary Science Letters*, *425*, 232–241. https://doi.org/10.1016/j.epsl.2015.05.044

Hofmann, M., & Rahmstorf, S. (2009). On the stability of the Atlantic meridional overturning circulation. *Proceedings of the National Academy of Sciences*, *106*(49), 20,584–20,589. https://doi.org/10.1073/pnas.0909146106

Howell, F. W., Haywood, A. M., Otto-Bliesner, B. L., Bragg, F., Chan, W. L., Chandler, M. A., et al. (2016). Arctic sea ice simulation in the PlioMIP ensemble. *Climate and Pastoralism*, *12*(3), 749–767. https://doi.org/10.5194/cp-12-749-2016

Liu, W., Liu, Z., & Brady, E. C. (2014). Why is the AMOC monostable in coupled general circulation models? *Journal of Climate*, *27*(6), 2427–2443. https://doi.org/10.1175/JCLI-D-13-00264.1

Liu, W., Xie, S. P., Liu, Z., & Zhu, J. (2017). Overlooked possibility of a collapsed Atlantic Meridional Overturning Circulation in warming climate. *Science Advances*, *3*(1), e1601666. https://doi.org/10.1126/sciadv.1601666

Madec, G., (2008). NEMO ocean engine. Note du Pole de modélisation 27, Institut Pierre-Simon Laplace (193 pp). Retrieved from http://www.nemo-ocean.eu/content/download/5302/31828/file/NEMO_book.pdf

Maier-Reimer, E., Mikolajewicz, U., & Crowley, T. (1990). Ocean general circulation model sensitivity experiment with an open Central American Isthmus. *Paleoceanography*, *5*, 349–366. https://doi.org/10.1029/PA005i003p00349

Manabe, S., & Stouffer, R. J. (1988). Two stable equilibria of a coupled ocean-atmosphere model. *Journal of Climate*, *1*(9), 841–866. https://doi.org/10.1175/1520-0442(1988)001<0841:TSEOAC>2.0.CO;2

Martínez-Botí, M. A., Foster, G. L., Chalk, T. B., Rohling, E. J., Sexton, P. F., Lunt, D. J., et al. (2015). Plio-Pleistocene climate sensitivity evaluated using high-resolution CO_2 records. *Nature*, *518*(7537), 49–54. https://doi.org/10.1038/nature14145

Mestas-Nuñez, A. M., & Molnar, P. (2014). A mechanism for freshening the Caribbean Sea in pre-Ice Age time. *Paleoceanography*, *29*, 508–517. https://doi.org/10.1002/2013PA002515

Molnar, P. (2008). Closing of the Central American Seaway and the Ice Age: A critical review. *Paleoceanography*, *23*, PA2201. https://doi.org/10.1029/2007PA001574

Montes, C., Cardona, A., Jaramillo, C., Pardo, A., Silva, J. C., Valencia, V., et al. (2015). Middle Miocene closure of the Central American seaway. *Science*, *348*(6231), 226–229. https://doi.org/10.1126/science.aaa2815

Otto-Bliesner, B. L., Jahn, A., Feng, R., Brady, E. C., Hu, A., & Löfverström, M. (2017). Amplified North Atlantic warming in the late Pliocene by changes in Arctic gateways. *Geophysical Research Letters*, *44*, 957–964. https://doi.org/10.1002/2016GL071805

Park, T., Park, W., & Latif, M. (2016). Correcting North Atlantic Sea surface salinity biases in the Kiel Climate Model: Influences on ocean circulation and Atlantic multidecadal variability. *Climate Dynamics*, *47*(7–8), 2543–2560. https://doi.org/10.1007/s00382-016-2982-1

Park, W., Keenlyside, N., Latif, M., Ströh, A., Redler, R., Roeckner, E., & Madec, G. (2009). Tropical Pacific climate and its response to global warming in the Kiel Climate Model. *Journal of Climate*, *22*(1), 71–92. https://doi.org/10.1175/2008jcli2261.1

Ravelo, A. C., & Andreasen, D. H. (2000). Enhanced circulation during a warm period. *Geophysical Research Letters*, *27*, 1001–1004. https://doi.org/10.1029/1999GL007000

Raymo, M. E., Grant, B., Horowitz, M., & Rau, G. H. (1996). Mid-Pliocene warmth: Stronger greenhouse and stronger conveyor. *Marine Micropaleontology*, *27*(1–4), 313–326. https://doi.org/10.1016/0377-8398(95)00048-8

Raymo, M. E., Ruddiman, W. F., Backman, J., Clement, B. M., & Martinson, D. G. (1989). Late Pliocene variation in northern hemisphere ice sheets and North Atlantic deep water circulation. *Paleoceanography*, *4*, 413–446. https://doi.org/10.1029/PA004i004p00413

Rind, D., & Chandler, M. (1991). Increased ocean heat transports and warmer climate. *Journal of Geophysical Research*, *96*, 7437–7461. https://doi.org/10.1029/91JD00009

Roeckner, E., Bäuml, G., Bonaventura, L., Brokopf, R., Esch, M., Giorgetta, M., et al. (2003). The atmospheric general circulation model ECHAM 5. PART I: Model description. Retrieved from http://pubman.mpdl.mpg.de/pubman/item/escidoc:995269/component/escidoc:995268/Report-349.pdf

Salau, O. R., Schneider, B., Park, W., Khon, V., & Latif, M. (2012). Modeling the ENSO impact of orbitally induced mean state climate changes. *Journal of Geophysical Research*, *117*, C06099. https://doi.org/10.1029/2012JC008265

Scaife, A. A., Copsey, D., Gordon, C., Harris, C., Hinton, T., & Keeley, S. (2011). Improved Atlantic winter blocking in a climate model. *Geophysical Research Letters*, *38*, L23703. https://doi.org/10.1029/2011GL049573

Stommel, H. (1961). Thermohaline convection with two stable regimes of flow. *Tellus*, *13*(2), 224–230. https://doi.org/10.3402/tellusa.v13i2.9491

Taylor, K. E., Stouffer, R. J., & Meehl, G. A. (2012). An overview of CMIP5 and the experiment design. *Bulletin of the American Meteorological Society*, *93*(4), 485–498. https://doi.org/10.1175/BAMS-D-11-00094.1

Thompson, R. S., & Fleming, R. F. (1996). Middle Pliocene vegetation: Reconstructions, paleoclimatic inferences, and boundary conditions for climate modeling. *Marine Micropaleontology*, *27*(1–4), 27–49. https://doi.org/10.1016/0377-8398(95)00051-8

Unger, N., & Yue, X. (2014). Strong chemistry-climate feedbacks in the Pliocene. *Geophysical Research Letters*, *41*, 527–533. https://doi.org/10.1002/2013GL058773

Valcke, S. (Ed.) (2006). OASIS3 user guide (prism_2-5). CERFACS Technical Report TR/CMGC/06/73, PRISM Report No 3 (60 pp.). Toulouse, France. Retrieved from http://www.prism.enes.org/Publications/Reports/oasis3_UserGuide_T3.pdf

Wang, C., Zhang, L., & Lee, S. K. (2014). A global perspective on CMIP5 climate model biases. *Nature Climate Change*, *4*(3), 201–205. https://doi.org/10.1038/nclimate2118

Zhang, X., Prange, M., Steph, S., Butzin, M., Krebs, U., Lunt, D. J., et al. (2012). Changes in equatorial Pacific thermocline depth in response to Panama seaway closure: Insights from a multi-model study. *Earth and Planetary Science Letters*, *317-318*, 76–84. https://doi.org/10.1016/j.epsl.2011.11.028

Zhang, Z., Nisancioglu, K. H., & Ninnemann, U. S. (2013). Increased ventilation of Antarctic deep water during the warm mid-Pliocene. *Nature Communications*, *4*, 1499. https://doi.org/10.1038/ncomms2521

Zubakov, V. A., & Borzenkova, I. I. (1988). Pliocene palaeoclimates: Past climates as possible analogues for mid-twenty-first century climate. *Palaeogeography Palaeoclimatology Palaeoecology*, *65*(1-2), 35–49. https://doi.org/10.1016/0031-0182(88)90110-1